Interfacial Phase Transitions in Block Copolymer/Homopolymer Blends

Kenneth R. Shull

IBM Almaden Research Center, 650 Harry Road, San Jose, California 95120-6099

Received October 26, 1992; Revised Manuscript Received January 21, 1993

ABSTRACT: A theoretical treatment of A–B diblock copolymer aggregation in matrices of homopolymer A is developed. These aggregates, termed "bulk" micelles when they form within a homogeneous matrix phase and "surface" micelles when they form at a surface or interface, can be pointlike (spherical), linear (cylindrical), or planar (lamellar). Bulk micelles set the limiting value of the copolymer chemical potential which can be obtained in a given system. Surface micelles will be formed at lower copolymer chemical potentials when the surface has a preferential affinity for the B repeat units which make up the micelle core. The interfacial properties are determined by the copolymer asymmetry g, the thermodynamic incompatibility χN_c between A and B copolymer blocks, the ratio N_h/N_c of the homopolymer and copolymer molecular weights, and a bare surface free energy difference $\gamma_a - \gamma_b$ between A and B polymers. A scaling treatment valid for $N_h/N_c \gtrsim 1$ is developed from a simple physical picture of the aggregation process. Phase transitions between different surface micellar geometries are predicted to occur for certain combinations of g and $\gamma_a - \gamma_b$. The primary result of the scaling treatment is a surface phase diagram describing the transitions which can occur for different values of these parameters. A more quantitative self-consistent-field treatment based on the description of the polymer chain statistics by a set of chain-end distribution functions is also developed. The self-consistent-field predictions include the detailed structures of both bulk and surface micelles and give values for the copolymer chemical potential for bulk micelles which are in quantitative agreement with recent experiments. The self-consistent-field theory is used to illustrate the detailed nature of some surface phase transitions and is also applied to the segregation of an A/B diblock copolymer to the interface between immiscible A and C homopolymers.

I. Introduction

The interfacial activity of block copolymers is largely responsible for the enormous amount of attention that these materials have received in recent years. Adsorption of diblock copolymer molecules to the solid/solution interface is perhaps the most well-known example of this interfacial activity.[1-3] Interactions between nonadsorbing blocks give rise to long-range repulsive forces[4] which play a dominant role in the behavior of colloidal dispersions.[5] The properties of polymer/polymer or polymer/nonpolymer interfaces can also be altered significantly by the addition of an appropriate block copolymer. Considerable increases in the adhesive strength of these interfaces have been obtained on addition of diblock copolymers.[6-8] Segregation of block copolymer molecules to the interface between immiscible homopolymers is also accompanied by a decrease in the interfacial tension. New equilibrium phases appear when the interfacial tension becomes vanishingly small.[9,10] The interfacial activity of block copolymers can be utilized in this way to create blend materials with unique properties.

It has generally been assumed that under equilibrium conditions block copolymers will adsorb to a surface to form a copolymer layer which is laterally homogeneous. This assumption is not necessarily valid, however, as argued by Ligoure in a recent theoretical treatment.[11] Here it was shown that under certain conditions very asymmetric diblock copolymers will adsorb from solution to form laterally heterogeneous "surface micelles". One expects that similar structures can be formed when the small-molecule solvent is replaced by a homopolymer, i.e., in block copolymer/homopolymer blends. Evidence for laterally heterogeneous surface structures in block copolymers and their mixtures with homopolymers can in fact be found in the recent electron microscopy study of Hasegawa and Hashimoto.[12] The focus of the present paper is on the different interfacial structures which can appear in block copolymer/homopolymer blends and on the phase transitions between these structures.

We study A/B diblock copolymers in an A homopolymer matrix. Adsorption of the B block to a surface is driven by the bare surface free energy difference $\gamma_a - \gamma_b$. The fundamental features of the adsorption process can be understood in terms of the wetting behavior of the B block.[11] An additional interface between A and B copolymer blocks is created when the copolymer adsorbs to the surface. Various interfacial phase transitions are possible when the B block does not completely wet the surface. The simple criterion for this nonwetting case is

$$\gamma_a - \gamma_b < \gamma_{ab} \tag{1}$$

where γ_{ab} is the free energy associated with an interface between A and B homopolymers, typically a few dyn/cm. Interfacial phase transitions are therefore expected for bare surface free energy differences on the order of 1 dyn/cm. One expects that this criterion can be met by careful selection of the substrate. Evidence for surface phase transitions exists, in fact, in recent adsorption measurements of polystyrene/poly(2-vinylpyridine) diblock copolymers from a polystyrene matrix, where the substrate was a self-assembled hydrocarbon layer supported on a silicon substrate.[13] One expects that eq 1 can also be satisfied for segregation of an A/B diblock copolymer to the interface between immiscible A and C homopolymers, depending on the relative thermodynamic interactions between A, B, and C segments.

The interfacial activity of a given block copolymer is determined by the copolymer chemical potential, which is in turn determined by the bulk phase behavior of the copolymer/homopolymer blend. We consider diblock copolymers, where this chemical potential is generally limited by the formation of micellar aggregates. As illustrated schematically in Figure 1a, these micelles, referred to here as "bulk micelles" to distinguish them the surface micelles mentioned above, can be spherical, cylindrical, or lamellar, depending on the copolymer

0024-9297/93/2226-2346$04.00/0

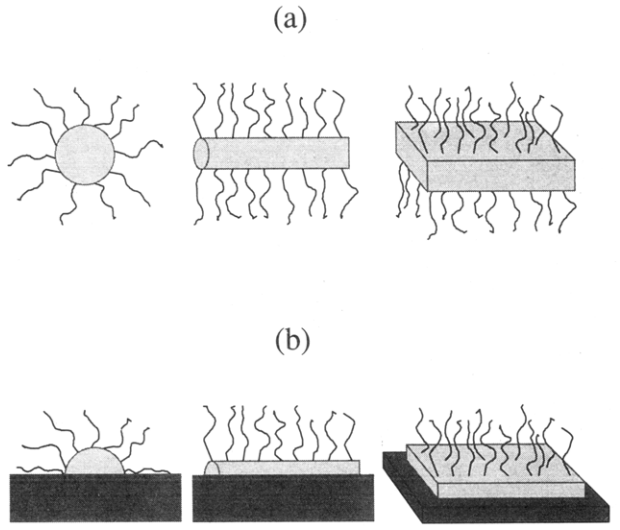

Figure 1. Schematic illustration of spherical, cylindrical, and lamellar micelles: (a) bulk micelles and (b) surface micelles.

asymmetry and on the ratio of homopolymer and copolymer molecular weights.[14-16] The first step in developing a theory of the interfacial activity of diblock copolymers is therefore to develop a theory of micellization. One can then apply a more generalized theory which includes an interface in order to determine which interfacial structures will be obtained at those accessible copolymer chemical potentials which do not exceed the maximum value corresponding to the formation of bulk micelles. These micelles can have axial or mirror symmetry within planes which are parallel to the interface, by analogy to spherical and cylindrical bulk micelles as shown in Figure 1b. Figure 1 also illustrates the correspondence between a bulk lamellar micelle and an absorbed layer which is homogeneous within a plane parallel to the interface. Note that surface micelles are not merely bulk micelles which have adsorbed to the surface. Surface micelles have the core region directly in contact with the surface and will form only when the surface has a preferential interaction with the core component of the micelle. An entropic driving force for surface or interface segregation of bulk micelles exists when N_h/N_c is high,[15,17,18] and one must be careful when interpreting the results of copolymer segregation experiments in terms of the formation of true surface micelles.

Two theoretical approaches are utilized in the present paper. A scaling theory of micellization, developed previously for bulk micelles,[17,19] is extended to surface micelles in section II. For lamellar micelles the treatment is similar in spirit to the earlier work of Marques *et al.*[20,21] on copolymer adsorption from solution. The scaling treatment more clearly illustrates the fundamental physics of the problem than does the detailed self-consistent-field (SCF) treatment of section III. However, quantitative predictions of the sort necessary to extract useful information from experimental data cannot be accurately obtained from a simple scaling treatment. For this reason the remaining sections of the paper are devoted to results obtained from the SCF treatment. Typical results are illustrated by considering an A/B diblock copolymer of degree of polymerization N_c in an A matrix homopolymer melt with this same degree of polymerization. These blends are characterized by the symmetry parameter g, defined as the ratio of volume of the B copolymer block to the volume of the entire copolymer chain, and by the Flory χ parameter characterizing the thermodynamic interaction between A and B repeat units. (The case g = 1 corresponds to a blend of A and B homopolymers and is treated briefly in the Appendix.) Sections IV and V are devoted to a discussion of an example diblock copolymer/homopolymer blend with $g = 0.2$ and $\chi N_c = 60$; bulk micelles are treated in section IV and surface micelles are treated in section V. These concepts are extended to polymer/polymer interfaces in section VI. The final section is a brief summary of our results.

II. Scaling Theory

In this section we develop a simplified scaling theory of micellization which illustrates the basic features expected for the surface properties of block copolymer/homopolymer blends. Because the chemical potential of block copolymer chains will be limited by the formation of micelles in the bulk homopolymer matrix phase, we must first have a model which predicts this chemical potential. Following an earlier treatment developed by Leibler for spherical micelles[19] and later extended to cylindrical and lamellar micelles,[17] we write down the free energy for a block copolymer micelle which forms in a high molecular weight homopolymer matrix as follows:

$$F_{\text{micelle}} = F_{\text{core}} + F_{\text{corona}} + F_{\text{interface}} \tag{2}$$

where F_{core}, F_{corona} and $F_{\text{interface}}$ represent the respective free energies corresponding to the micelle core, the micelle corona, and the interface between the core and corona. The free energy of the micelle core is given by the stretching free energy of chains in the micelle:

$$F_{\text{core}}/k_BT = QK(R_{\text{core}}{}^2/gN_ca^2) \tag{3}$$

where Q is the number of chains in the micelle, R_{core} is the radius of the micelle core (taken as half the core thickness for lamellar micelles), and a is the statistical segment length of a repeat unit, defined such that the copolymer radius of gyration R_g is given by $a(N_c/6)^{1/2}$. The constant K is equal to 0.370 for spherical micelles, 0.616 for cylindrical micelles, and 1.234 for lamellar micelles.[22] The corona free energy arises from the entropic stretching of the corona block, taking into account the variation in chain stretching with distance away from the core/corona interface:

$$\frac{F_{\text{corona}}}{k_BT} = \frac{3Q}{2a^2}\int_{R_{\text{core}}}^{R} \mathrm{d}r \left(\frac{\mathrm{d}r}{\mathrm{d}n}\right) \tag{4}$$

where n varies from 0 at the core/corona interface to $(1 - g)N_c$ at the outer edge of the corona, and R is the total micelle radius. Swelling of the corona by the homopolymer matrix chains has been neglected in eq 4. This approximation restricts the validity of our scaling treatment to homopolymer molecular weights which are at least equal to the molecular weight of the corona block of the copolymer chain. This criterion is based on previous calculations which show that, for a planar geometry, swelling of a polymer "brush" becomes important only for homopolymer molecular weights which are less than the brush molecular weight.[18] These calculations are relevant here because the corona of a block copolymer micelle can be viewed as a brush. The failure of high molecular weight homopolymer chains to significantly swell the micelle corona can be attributed to the $1/N$ dependence of the entropy of mixing for homopolymer chains within a micelle corona and is not a feature which is unique to a planar geometry.[23] Therefore, the basic swelling criterion as derived for a planar geometry is not expected to be significantly altered by a transformation to a cylindrical or spherical geometry.

The interfacial free energy has a contribution from the free energy of interaction between the immiscible A and

B repeat units across the interface and a second contribution from the localization of the junctions between A and B copolymer blocks to this narrow interfacial region:

$$F_{\text{interface}} = A_{\text{core}}\gamma_{\text{ab}} + Q\delta F_{\text{loc}} \quad (5)$$

where A_{core} is the area of the core/corona interface and ΔF_{loc} is the entropic joint localization penalty per chain. (Earlier developments of the theory[17,19] which do not include the joint localization term ΔF_{loc} underestimate the free energy per chain in a micelle.) For γ_{ab} we use the interfacial free energy γ_∞ for homopolymers of infinite molecular weight:[24]

$$\gamma_{\text{ab}} \approx \gamma_\infty = a\rho_0 k_B T(\chi/6)^{1/2} \quad (6)$$

The joint localization term ΔF_{loc} for end-functionalized chains has been shown to have the following form:[18]

$$\Delta F_{\text{loc}} = 1.1 k_B T \ln(R_g^{\,b}/\delta_s) \quad (7)$$

where $R_g^{\,b}$ is the radius of gyration of the end-functionalized chain and δ_s is the width of the region in which the end is confined. As an estimate for δ_s we use the interfacial width which one obtains for homopolymers with $\chi N = \infty$:[24]

$$\delta_s = 2a(6\chi)^{1/2} \quad (8)$$

Diblock copolymer chains actually consist of two separate brushes, corresponding to each of the two blocks. As a rough approximation to the actual joint localization term, we will consider the contributions from both blocks simultaneously by using the overall copolymer radius of gyration in the expression for the joint localization term. This approach is reasonable, given the other approximations made in the simple scaling treatment. The following expression is obtained for the joint localization term by substitution of $2a(6\chi)^{1/2}$ for δ_s and R_g ($R_g = a(N_c/6)^{1/2}$) for $R_g^{\,b}$:

$$\Delta F_{\text{loc}} = 0.55 k_B T \{\ln(\chi N_c) - 0.76\} \quad (9)$$

Semenov has obtained a slightly different form of the joint localization term which, although not a unique function of χN_c, is expected to be more accurate for lamellar micelles.[22] Differences between the two forms for ΔF_{loc} are relatively minor, however, and there is no clear advantage to be gained from the use of the more complicated form, especially when applied to spherical and cylindrical micelles.

The free energy per copolymer chain F_{micelle}/Q can be expressed entirely in terms of R by using the appropriate geometric relationships between R, R_{core}, and A_{core} and between r and dr/dn.[17,19] The copolymer chemical potential $\mu_c = \partial F_{\text{micelle}}/\partial Q$ can also be obtained as a function of R. Figure 2a shows μ_c and F_{micelle}/Q as a function of the micelle radius for a spherical copolymer micelle with g = 0.2 and $\chi N_c = 60$. The equilibrium micelle radius R^b_{cmc} and the critical copolymer chemical potential μ^b_{cmc} for the formation of bulk micelles is given by the minimum in F/Q, which occurs at the intersection of the curves for F/Q and μ_c. For spherical micelles with $g = 0.2$ and $\chi N_c = 60$, the intersection point gives $R^b_{\text{cmc}} = 2.89R_g$ and $\mu^b_{\text{cmc}} = 5.62k_BT$. The intersection of the curves at this point is a statement of the fact that copolymer micelles appear when the excess free energy of a micelle is zero; i.e., $F_{\text{micelle}} - Q\mu_c = 0$.

The R dependence of F_{micelle} can be used to determine the activation free energy for micelle formation. The free energy change associated with the formation of a micelle is given by $\Delta F_{\text{micelle}}(R) = F_{\text{micelle}}(R) - Q\mu_c$, where Q and R are related through the space-filling constraint ($4\pi R^3/3 = Qv$ for spherical micelles, where v is the volume of a copolymer chain). The two values of R which correspond to a given copolymer chemical potential represent a maximum (the lower value of R) and a minimum (the higher value of R) in $\Delta F_{\text{micelle}}$. These features are illustrated here by consideration of the cases where $\mu_c = \mu^b_{\text{cmc}}$, $\mu_c = 6k_BT$, and $\mu_c = 7k_BT$. These values of μ_c are represented by the three dotted lines in Figure 2a. Figure 2b shows the R dependence of $\Delta F_{\text{micelle}}$ for each of these values of μ_c. In each case $\Delta F_{\text{micelle}}$ passes through a maximum where the appropriate dotted line first meets the dashed curve in Figure 2a. This maximum value of $\Delta F_{\text{micelle}}$, corresponding to the activation free energy $\Delta F^*_{\text{micelle}}$ of a micelle, is strongly dependent on μ_c and can be quite large. If the statistical segment is defined such that $N_c a^3 = v$, the normalization factor R_g^3/v is equal to $0.068\sqrt{N}$. Thus for $N = 1000$ the activation free energy for the formation of a spherical micelle with $\chi N = 60$ and $g = 0.2$ is equal to $23k_BT$ for $\mu_c = 7k_BT$, $38k_BT$ for $\mu_c = 6k_BT$, and $46k_BT$ for $\mu_c = \mu^b_{\text{cmc}} = 5.62k_BT$. The equilibrium copolymer chemical potential at which micelles form is the value which has $\Delta F_{\text{micelle}} = 0$ at the minimum value, as illustrated in Figure 2b.

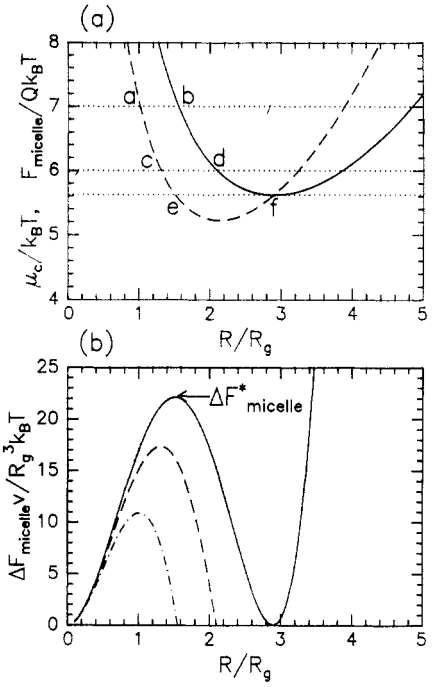

Figure 2. Scaling predictions for a spherical bulk micelle with $g = 0.2$ and $\chi N = 60$: (a) Copolymer chemical potential (– –) and free energy per chain (—). The significance of the letters and dotted lines is described in the text. (b) Excess free energy of a micelle for $\mu_c = \mu^b_{\text{cmc}} = 5.62k_BT$ (—), $\mu_c = 6k_BT$ (– –), and $\mu_c = 7k_BT$ (– · –).

Because the activation energies associated with micelle formation are so large, the "effective" copolymer chemical potential in a real system may exceed the true equilibrium value.[25] The process by which equilibrium is approached in a blend which is supersaturated with free copolymer chains occurs as follows. Suppose the chemical potential of copolymer chains in the blend system described in Figure 2 is $7k_BT$. Micelles will form in this system in a rate controlled by the R dependence of $\Delta F_{\text{micelle}}$ as given by the lowest of the three curves on Figure 2b. A stable micelle "nucleus" is formed when the copolymer chemical potential in the micelle is equal to $7k_BT$ (point A in Figure 2a). Because the chemical potential of copolymer chains is a decreasing function of the micelle radius in this regime,

the overall free energy of the system will be decreased whenever a copolymer chain is removed from the bulk reservoir and inserted into the micelle. Any micelles which have reached the critical size for stability will therefore grow until the chemical potential of copolymer chains in the micelle is again equal to the chemical potential of copolymer chains in the bulk matrix phase. Micelle growth will be determined by diffusion of copolymer chains to a micelle and by the rate of insertion of individual chains into a micelle. A micelle nucleus formed from a reservoir of copolymer chains with $\mu_c = 7k_BT$ will grow at a rate determined by these factors and will eventually reach the final size given by point B in Figure 2a. This point corresponds to a minimum in $\Delta F_{micelle}$, whereas point A corresponds to a maximum in $\Delta F_{micelle}$. As more and more micelles form, the reservoir will be depleted and the copolymer chemical potential will decrease. When the copolymer chemical potential is equal to $6k_BT$, new micelles will form at point C. The activation free energy and the critical micelle size are now higher, and the rate of micelle formation will be decreased. The final size of the micelles as given by point D will be decreased as well. The micelle size distribution is expected to be relatively narrow at all times, however, because the larger micelles formed earlier in the process shrink to equilibrate with the lower effective copolymer chemical potential in the system. Eventually a true equilibrium will be approached, where micelles nucleate with a size given by point E and grow to a size equal to R^b_{cmc}, as given by point F. These equilibrium structures are the focus of the remainder of this paper.

The following analytical expressions can be obtained for the equilibrium copolymer chemical potentials ($\mu^b_{cmc\text{-}s}$, $\mu^b_{cmc\text{-}c}$, $\mu^b_{cmc\text{-}l}$) and equilibrium radii ($R^b_{cmc\text{-}s}$, $R^b_{cmc\text{-}c}$, $R^b_{cmc\text{-}l}$) for spherical, cylindrical, and lamellar micelles which form in the bulk homopolymer matrix phase:

spherical bulk micelles

$$\mu^b_{cmc\text{-}s}/k_BT = 1.72(\chi N_c)^{1/3}g^{4/9}(1.74g^{-1/3} - 1)^{1/3} + 0.55\ln(\chi N_c) - 0.76 \quad (10)$$

$$R^b_{cmc\text{-}s}/R_g = 2.62(\chi N_c)^{1/6}g^{1/3}(1.74 - g^{1/3})^{-1/3} \quad (11)$$

cylindrical bulk micelles

$$\mu^b_{cmc\text{-}c}/k_BT = 1.19(\chi N_c)^{1/3}g^{1/3}(1.64 - \ln g)^{1/3} + 0.55\ln(\chi N_c) - 0.76 \quad (12)$$

$$R^b_{cmc\text{-}c}/R_g = 2.52(\chi N_c)^{1/6}g^{1/6}(1.65 - \ln g)^{-1/3} \quad (13)$$

lamellar bulk micelles

$$\mu^b_{cmc\text{-}l}/k_BT = 0.67(\chi N_c)^{1/3}(5.64 - g)^{1/3} + 0.55\ln(\chi N_c) - 0.76 \quad (14)$$

$$R^b_{cmc\text{-}l}/R_g = 2.25(\chi N_c)^{1/6}(5.64 - g)^{-1/3} \quad (15)$$

If the repeat units which make up the micellar core have a preferential interaction with a surface, then surface micelles (Figure 1b) will appear at lower copolymer chemical potentials than bulk micelles. A very simple picture of this surface micellization process can be obtained by assuming that the micellar geometry is not strongly perturbed by the surface. (The validity of this approximation in a qualitative sense is in fact verified by the SCF calculations of section V.) In this case a surface micelle corresponds to a bulk micelle which has been cut precisely in half. Surface micelles with axial or mirror symmetry (the first two geometries shown in Figure 1b) will be hemispheres and half-cylinders, respectively. The tendency for surface micelles to adopt a spherical, cylindrical, or lamellar geometry will depend on the copolymer asymmetry and the strength of the surface interaction. We let A' represent the contact area of the overall micelle with the surface and A'_{core} represent the contact area of the micelle core with the surface. The free energy per chain in a surface micelle will be reduced from the value of $F_{micelle}/Q$ in a bulk micelle of the corresponding geometry by the quantity $(\gamma_a - \gamma_b)A'_{core}/Q$, where γ_a and γ_b are the respective surface free energies of A and B polymers. One has $A'_{core} = A'$ for lamellar micelles, $A'_{core} = 2R_{core}l$ for cylindrical micelles of length l, and $A'_{core} = \pi R_{core}^2$ for spherical micelles. The analysis is identical to that presented above for micelles which form in the bulk matrix phase, with the subtraction of $(\gamma_a - \gamma_b)A'_{core}/Q$ from the expression for $F_{micelle}/Q$. The following relationships are obtained for the copolymer chemical potentials ($\mu^s_{cmc\text{-}s}$, $\mu^s_{cmc\text{-}c}$, $\mu^s_{cmc\text{-}l}$) and equilibrium radii ($R^s_{cmc\text{-}s}$, $R^s_{cmc\text{-}c}$, $R^s_{cmc\text{-}l}$) for spherical, cylindrical, and lamellar surface micelles:

spherical surface micelles

$$\mu^s_{cmc\text{-}s} - \Delta F_{loc} = (\mu^b_{cmc\text{-}s} - \Delta F_{loc})\{1 - 0.25((\gamma_a - \gamma_b)/\gamma_{ab})\}^{2/3} \quad (16)$$

$$R^s_{cmc\text{-}s} = R^b_{cmc\text{-}s}\{1 - 0.5((\gamma_a - \gamma_b)/\gamma_{ab})\}^{1/3} \quad (17)$$

cylindrical surface micelles

$$\mu^s_{cmc\text{-}c} - \Delta F_{loc} = (\mu^b_{cmc\text{-}c} - \Delta F_{loc})\{1 - 0.318((\gamma_a - \gamma_b)/\gamma_{ab})\}^{2/3} \quad (18)$$

$$R^s_{cmc\text{-}c} = R^b_{cmc\text{-}c}\{1 - 0.636((\gamma_a - \gamma_b)/\gamma_{ab})\}^{1/3} \quad (19)$$

lamellar surface micelles

$$\mu^s_{cmc\text{-}l} - \Delta F_{loc} = (\mu^b_{cmc\text{-}l} - \Delta F_{loc})\{1 - (\gamma_a - \gamma_b)/\gamma_{ab}\}^{2/3} \quad (20)$$

$$R^s_{cmc\text{-}l} = R^b_{cmc\text{-}l}\{1 - (\gamma_a - \gamma_b)/\gamma_{ab}\}^{1/3} \quad (21)$$

The surface (or interfacial) free energy γ corresponding to a surface covered with adsorbed copolymer chains can be written in the following form:

$$\gamma = \gamma_a + \left\{\frac{F_{micelle}}{Q} - \mu_c\right\}\frac{Q}{A} \quad (22)$$

Here A is the area per surface micelle, equal to A' for lamellar and cylindrical surface micelles, and equal to $1.103A'$ for an assumed hexagonal packing of spherical surface micelles. The first term in eq 22 represents the surface free energy of an A homopolymer melt in the absence of copolymer segregation, and the second term represents the change in surface energy associated with the formation of the adsorbed layer. Note that this change in free energy is given by multiplying the excess free energy per copolymer chain by the areal density of copolymer chains in the adsorbed copolymer layer. The above equations for the critical values of the copolymer chemical potential at the onset of surface micellization were obtained by setting $\gamma = \gamma_a$ or, alternatively, $F_{micelle}/Q - \mu_c = 0$ as described above. When $\gamma_a - \gamma_b = 0$, surface micelles are predicted to appear at the same copolymer chemical potential as do bulk micelles of the corresponding geometry. As previously calculated, spherical micelles are

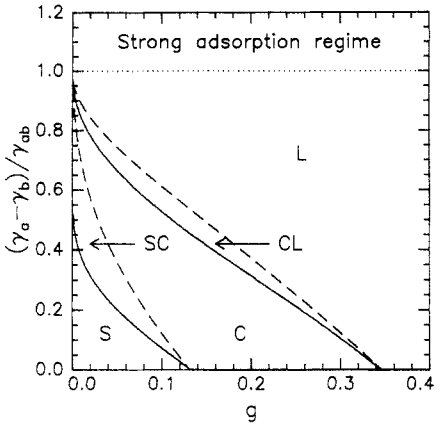

Figure 3. Surface phase diagram showing the regions where different surface morphologies are possible. Dashed lines separate regions where different geometries are the first to form; spherical surface micelles form first in regions S and SC, cylindrical surface micelles form first in regions C and CL, and lamellar surface micelles form first in region L. Solid lines separate regions where different geometries have the lowest free energy at the limiting copolymer chemical potential corresponding to the formation of bulk micelles. These are spheres in region S, cylinders in regions SC and C, and lamellae in regions CL and L. The dotted line defines the onset of the strong segregation regime where transitions in the adsorption isotherm are no longer present.

predicted for $g < 0.13$, cylindrical micelles are predicted for $0.13 < g < 0.35$, and lamellar micelles are predicted for $g > 0.35$.[17] For $\gamma_a - \gamma_b > 0$, surface micelles appear at copolymer chemical potentials below the limiting values corresponding to the formation of bulk micelles. In this case there will be a window of copolymer chemical potentials for which surface micelles will exist. The largest attainable copolymer chemical potential is determined by the formation of bulk micelles. This maximum chemical potential μ^b_{cmc} is given by eq 10 for $g < 0.13$, eq 12 for $0.13 < g < 0.35$ and eq 14 for $g > 0.35$.

Figure 3 is a "surface phase diagram" that illustrates which surface micellar geometries are possible for different combinations of g and $\gamma_a - \gamma_b$. The dashed lines separate the diagram into regions where spherical, cylindrical, or lamellar surface micelles have the lowest value of μ^s_{cmc}. Solid lines separate the phase diagram into regions where these different geometries minimize the overall surface free energy at the limiting copolymer chemical potential μ^b_{cmc} corresponding to the formation of bulk micelles. Areal densities of copolymer chains in the different surface micelles are obtained from the appropriate incompressibility constraints, i.e., $Qv = AR$ for lamellar micelles, $Qv/0.5\pi R^2 l = A/2Rl$ for cylindrical micelles, and $Qv/(^4/_6\pi R^3) = 0.907A/\pi R^2$ for spherical micelles. The factor of 0.907 in the incompressibility condition for spherical surface micelles is due to the assumed hexagonal packing of these micelles. The regions marked S, C, and L in Figure 3 are the respective regions where spherical, cylindrical, or lamellar micelles have the lowest value of μ^s_{cmc} and the lowest value of γ for all copolymer chemical potentials between μ^s_{cmc} and μ^b_{cmc}. No phase transitions between different surface micellar geometries are expected in these regions. A surface phase transition from spheres to cylinders is predicted in region SC as the copolymer chemical potential is increased from μ^s_{cmc} toward μ^b_{cmc}. A similar surface phase transition from cylinders to lamellae is predicted in region CL. The copolymer chemical potentials at which these transitions occur are obtained by equating the values of γ for the appropriate geometries.

Adsorption isotherms for characteristic points lying within the different regions of the surface phase diagram

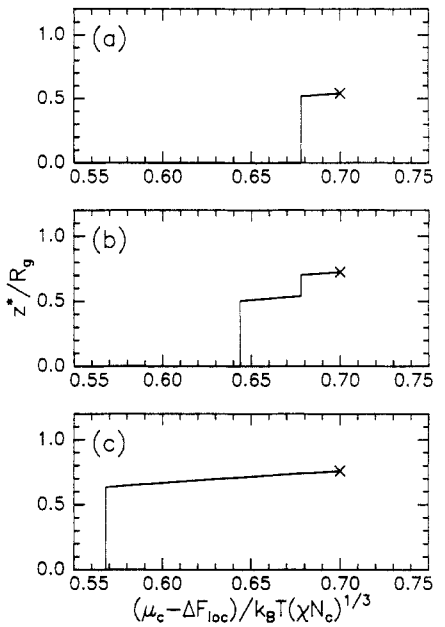

Figure 4. Adsorption isotherms as calculated by the scaling theory for a series of systems with $g = 0.05$: (a) $(\gamma_a - \gamma_b)/\gamma_{ab} = 0.05$ (region S); (b) $(\gamma_a - \gamma_b)/\gamma_{ab} = 0.25$ (region SC); (c) $(\gamma_a - \gamma_b)/\gamma_{ab} = 0.50$ (region C).

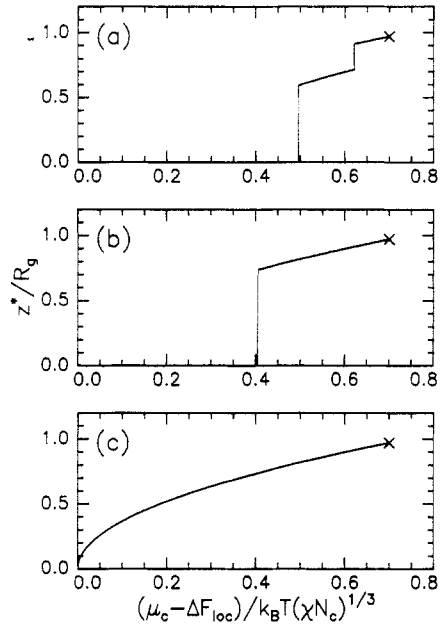

Figure 5. Adsorption isotherms as calculated by the scaling theory for a series of systems with $g = 0.05$: (a) $(\gamma_a - \gamma_b)/\gamma_{ab} = 0.70$ (region CL); (b) $(\gamma_a - \gamma_b)/\gamma_{ab} = 0.80$ (region L); (c) $(\gamma_a - \gamma_b)/\gamma_{ab} > 1$ (region L, strong adsorption regime).

are shown in Figures 4 and 5. The adsorbed amount is plotted as the surface excess z^*_c, equal to vQ/A. All six isotherms shown in these figures are for $g = 0.05$, with $(\gamma_a - \gamma_b)/\gamma_{ab}$ varying from 0.1 (Figure 4a) to 1.0 (Figure 5c). Spherical bulk micelles are favored for this low value of g, and the normalized value of μ^b_{cmc} is 0.700. As $(\gamma_a - \gamma_b)/\gamma_{ab}$ is increased from zero, μ^s_{cmc} is decreased from μ^b_{cmc} in accordance with eqs 16, 18, and 20. For $(\gamma_a - \gamma_b)/\gamma_{ab} = 0.10$ spherical surface micelles have the lowest free energy over the entire range between μ^s_{cmc} and μ^b_{cmc} and the normalized value of μ^s_{cmc} is 0.678. This combination of g and $(\gamma_a - \gamma_b)/\gamma_{ab}$ lies within the region denoted by S in the surface phase diagram shown in Figure 3. In this region there is a single transition to a spherical surface morphology in the adsorption isotherm. When $(\gamma_a - \gamma_b)/\gamma_{ab}$ is increased to 0.25, one enters the region of the phase diagram marked

SC, and two surface phase transitions are observed as illustrated in Figure 4b. The first transition is to a spherical surface morphology and the second transition is to a cylindrical morphology. Typical adsorption isotherms for points lying within regions C, CL, and L are shown in Figure 4c and parts a and b of Figure 5, respectively.

For $\gamma_a - \gamma_b > \gamma_{ab}$, there is no longer a penalty for the formation of a copolymer-rich layer at the interface. In this "strong adsorption" regime there will be no transitions in the copolymer adsorption isotherm. Instead there will be a continuous increase in the adsorbed amount with increasing copolymer chemical potential as illustrated in Figure 5c. Equations 3 and 4 for the core and corona free energies were derived from the assumption that the polymer chains were strongly stretched, a condition which requires $R > R_g$. The approximations upon which the scaling theory is based therefore deteriorate as the quantity $(\gamma_a - \gamma_b)/\gamma_{ab}$ approaches 1, because eq 21 has R^s_{cmc} approaching zero in this limit. The scaling prediction that there is some limiting value of $\gamma_a - \gamma_b$ above which there will be no interfacial phase transitions remains valid, however, even if the magnitude of the critical value of this quantity is in error. At low coverages the copolymer chemical potential in the adsorbed copolymer layer will be determined by the two-dimensional entropy of mixing of copolymer chains at the interface. Inclusion of this entropy of mixing term in the scaling analysis allows one to extend the results to copolymer chemical potentials which are less than zero.[19,26] Quantitative predictions cannot be obtained by such a scaling model, however. In addition, the scaling treatment gives no information with regard to the more detailed structure of the interfacial layer. We use the simple scaling picture to illustrate the basic features of the adsorption and micellization processes. Detailed features of these processes are more adequately described by the self-consistent-field theory as described in the following sections.

III. Self-Consistent-Field (SCF) Theory

The free energy density f_0 of a homogeneous mixture of polymers is given in the Flory approximation by the following simple formula:

$$\frac{f_0}{k_B T \rho_0} = \sum_k \phi_k \ln \phi_k + \frac{1}{2}\sum_{m \neq n} \chi_{mn}\phi_m\phi_n \qquad (23)$$

where ϕ_k is the volume fraction of component k and χ_{mn} is the Flory interaction parameter characterizing the thermodynamic interaction between m and n repeat units. The quantity ρ_0 is the number density of polymer repeat units and defines the reference volume for the interaction parameters. The chemical potentials can be obtained from eq 23 with the use of the following formula:[27]

$$\frac{\mu_k}{N_k} = \frac{\partial(f/\rho_0)}{\partial\phi_k} + f/\rho_0 - \sum_k \phi_k \frac{\partial(f/\rho_0)}{\partial\phi_k} \qquad (24)$$

where the derivative with respect to ϕ_k is taken with all other ϕ's held constant. Combination of eqs 23 and 24 gives[28]

$$\frac{\mu_k}{k_B T} = \ln \phi_k + 1 - N_k K_\phi + \frac{1}{k_B T}\sum_{j=1}^{N_k} w^\circ(p(j)) \qquad (25)$$

with

$$K_\phi = \sum_k \frac{\phi_k}{N_k} \qquad (26)$$

and

$$\frac{w^\circ(p)}{k_B T} = \frac{1}{2}\sum_{m \neq n} \{\phi_m - \delta(m-p)\}\chi_{mn}\{\phi_n - \delta(n-p)\} \qquad (27)$$

Here ϕ_m represents the overall volume fraction of the chemical species m, and the summation is over all possible species (A, B, C, etc.). The δ functions are defined so that $\delta(m-p) = 1$ for $m = p$ and $\delta(m-p) = 0$ for $m \neq p$. For a system with only a and b repeat units one obtains $w^\circ(a)/k_B T = \chi_{ab}\phi_b^2$ and $w^\circ(b)/k_B T = \chi_{ab}\phi_a^2$. The first three terms on the right side of eq 25 are associated with the logarithmic entropy of mixing term in the free energy expression. The last term in eq 25 is associated with the interaction parameters, which are assumed to be independent of the composition. A compositional dependence of these parameters will give rise to a more complicated version of eq 25. The reference state for which $\mu_k = 0$ is a pure homopolymer melt with a degree of polymerization of N_k.

Equations 23–25 specify the properties of the bulk coexisting phases but say nothing of the interfacial properties. Consideration of these interfacial properties requires that one introduces a mechanism for the treatment of spatial inhomogeneities. The SCF treatment is based on the description of polymer chain statistics by distribution functions $q_k(\mathbf{r},j)$. Here j is an index which runs from unity at one end of a polymer chain to N_k at the other end of a chain. Two distinct distribution functions, $q_{k1}(\mathbf{r},j)$ and $q_{k2}(\mathbf{r},j)$, are required whenever the two ends are distinct, as with diblock copolymers. The quantity $q_{k1}(\mathbf{r},j)$ is proportional to the probability that the jth repeat unit (measured from the appropriate end of the block copolymer) exists at $\mathbf{r}$. Volume fractions corresponding to the different repeat units are obtained from the requirement that a repeat unit which is j units away from one end of the chain must by $N_k - j$ units away from the other end of the chain. The volume fraction $\phi_k(\mathbf{r},j)$ corresponding to the jth repeat unit along a polymer chain is therefore proportional to the product of $q_{k1}(\mathbf{r},j)$ and $q_{k2}(N_k-j)$. After the appropriate normalization,[18,29,30] we obtain

$$\phi_k(\mathbf{r},j) = \frac{1}{N_k}\exp(\mu_k/k_B T - 1) q_{k1}(\mathbf{r},j)\, q_{k2}(\mathbf{r},N_k-j) \qquad (28)$$

The volume fraction of any given portion of a polymer chain is given by the summation over the appropriate repeat units. The volume fraction of polymer k, for example, is given by the summation of all N_k repeat units:

$$\phi_k(i) = \sum_{j=1}^{N_k} \phi_k(i,j) = \frac{1}{N_k}\exp(\mu_k/k_B T - 1)\sum_{j=1}^{N_k} q_{k1}(i,j)\, q_{k2}(i,N-j) \qquad (29)$$

We impose a discretization scheme similar to that used by Scheutjens and Fleer[31,32] so that the position $\mathbf{r}$ is represented by the integral coordinates i_1, i_2, and i_3. The distance between the two adjacent layers is the segment length a defined so that the polymer radius of gyration R_g is given by $a(N_k/6)^{1/2}$. We assume here that all components have the same segment length a, although the equations are easily generalized to situations where these segment lengths differ.[33] Connectivity of the polymer chains is accounted for in the recursion relations for q_{k1} and q_{k2}. In systems with planar, cylindrical, or spherical symmetry all quantities are functions of only a single coordinate i, and the problem is simplified enormously. For these highly

symmetric cases the recursion relationships can be written as follows:

$$q_{k1}(i,j) = \{\lambda_{-1}q_{k1}(i-1,j-1) + \lambda_0 q_{k1}(i,j-1) + \lambda_{+1}q_{k1}(i+1,j-1)\}\exp\{-w(i,j)/k_BT\} \quad (30)$$

$$q_{k2}(i,j) = \{\lambda_{-1}q_{k2}(i-1,j-1) + \lambda_0 q_{k2}(i,j-1) + \lambda_{+1}q_{k2}(i+1,j-1)\}\exp\{-w(i,j)/k_BT\} \quad (31)$$

with $q_{k1}(i,0) = q_{k2}(i,0) = 1$.

Equations 30 and 31 are statements of the requirement that a chain segment of length $j-1$ be adjacent to a chain segment of length j. The transition probabilities λ_{-1}, λ_0, and λ_{+1} represent the respective fractions of nearest-neighbor sites which lie in layer $i-1$, i, or $i+1$, with the reference site being in layer i. A simple cubic lattice has four nearest-neighbor sites in the same layer as the reference site and one nearest neighbor in each of the neighboring layers. For planar symmetry one therefore obtains $\lambda_{+1} = \lambda_{-1} = {}^1/_6$ and $\lambda_0 = {}^4/_6$. Leermakers and Scheutjens obtain the transition probabilities for systems with spherical or cylindrical symmetry by assuming that λ_{+1} and λ_{-1} are proportional to the contact areas between the appropriate layers:[34]

$$\lambda_{-1}(i) = \frac{1}{6}S(i-1)/L(i) \quad (32)$$

$$\lambda_{+1}(i) = \frac{1}{6}S(i)/L(i) \quad (33)$$

where $S(i)$ is the surface area between layers i and $i-1$ and $L(i)$ is number of lattice sites within layer i. For a spherical geometry $S(i) = 4\pi i^2$ and for a cylindrical geometry $S(i) = 2\pi il$, where l is the length of the cylinder. The number of lattice sites in layer i is given by the difference in total volumes V for systems with i and $i-1$ layers:

$$L(i) = V(i) - V(i-1) \quad (34)$$

with $V(i) = (4/3)\pi i^3$ for the spherical geometry and $V(i) = \pi i^2 l$ for the cylindrical geometry. The remaining transition probability is obtained from the requirement that all three probabilities sum to 1:

$$\lambda_0(i) = 1 - \lambda_{-1}(i) - \lambda_{+1}(i) \quad (35)$$

Equations 30–35 form a discrete representation of the modified diffusion equation introduced by Edwards[35] and used in a large number of previous theoretical treatments.[24,29,30,36–39] For one-dimensional problems where q and w are functions of a single spatial variable r the modified diffusion equation has the following form:

$$\frac{\partial q(r,j)}{\partial j} = \frac{a^2}{6}\left\{\frac{\partial^2 q(r,j)}{\partial r^2} + \frac{C}{r}\frac{\partial q(r,j)}{\partial r}\right\} - w(r)\,q(r,j) \quad (36)$$

where $C = 0$ for systems with planar symmetry, $C = 1$ for systems with cylindrical symmetry, and $C = 2$ for systems with spherical symmetry. The relationship between eq 36 and eqs 30 and 31 has been derived previously for the case of planar symmetry.[18] Extension of this relationship to the spherically and cylindrically symmetric cases is straightforward.

Laterally heterogeneous surface structures are of particular interest in our current work. In this case the properties vary in the direction normal to the interface as well as within the plane of the interface, and the problem is no longer one-dimensional. In the most general situation the distribution functions and mean fields will be functions of three coordinates. We assume that there is an additional symmetry in the x–y plane (with z being the direction normal to the interface) which allows us to use only two coordinates represented by the indices i_1 and i_2. Here i_1 is associated with the z coordinate and identifies the distance of a given site from the interface. The index i_2 identifies the distance of a given site from a center of symmetry which can be either a line (axial symmetry) or a plane (mirror symmetry). As with the one-dimensional problems, the recursion relationships for the distribution functions are derived from the transition probabilities between sites on the appropriate lattice, with the added complication that there are now five distinct transition probabilities instead of the original three. The probability for transitions between adjacent layers oriented parallel to the surface (characterized by i_1) is equal to ${}^1/_6$, just as it is for the one-dimensional case with planar symmetry. We now have three distinct transitions within one of these layers however, i.e., those where i_2 decreases by 1, whose where i_2 remains constant, and those where i_2 increases by 1. The respective probabilities for these three transitions are λ'_{-1}, λ'_0, and λ'_{+1}, from which we obtain the following recursion relation for q_{k1}:

$$q_{k1}(i_1,i_2,j) = \Big\{\lambda'_{-1}q_{k1}(i_1,i_2-1,j-1) + \lambda'_0 q_{k1}(i_1,i_2,j-1) + \lambda'_{+1}q_{k1}(i_1,i_2+1,j-1) + \frac{1}{6}q_{k1}(i_1-1,i_2,j-1) + \frac{1}{6}q_{k1}(i_1+1,i_2,j-1)\Big\}\exp\{-w(i_1,i_2,j)/k_BT\} \quad (37)$$

with an analogous equation for q_{k2} and all distribution functions initialized to 1 at $j = 0$. A Cartesian coordinate system is used to derive λ'_{-1}, λ'_0, and λ'_{+1} for systems with mirror symmetry in the x–y plane. In this case the x–y plane is a square lattice, with a given site having four nearest-neighbor sites. Two of these neighboring sites have the same value of i_2 as the reference site, a third site has i_2 increased by 1, and the fourth site has i_2 decreased by 1. The three additional transition probabilities for this symmetry class are therefore $\lambda'_{-1} = \lambda'_{+1} = {}^1/_6$ and $\lambda'_0 = {}^1/_3$. For the axially symmetric case the x–y plane is broken up into a series of concentric circles centered around $i_2 = 0$. The probabilities for transitions between these layers are the same as those already given for the cylindrically symmetric case:

$$\lambda'_{-1}(i_2) = \frac{1}{6}S(i_2-1)/L(i_2) \quad (38)$$

$$\lambda_{+1}(i_2) = \frac{1}{6}S(i_2)/L(i_2) \quad (39)$$

with $S(i_2) = 2\pi i_2$ and $L(i_2) = \pi i_2^2 - \pi(i_2-1)^2$. The remaining transition probability is obtained from the requirement that all transition probabilities sum to 1:

$$\lambda'_0(i) = 4/6 - \lambda'_{-1}(i) - \lambda'_{+1}(i) \quad (40)$$

The mean fields $w(\mathbf{r},j)$ are functions of the local composition and of the repeat unit represented by j. The j dependence of the mean fields is taken into account through the expanded notation $w(i,p(j))$, where p designates the type of repeat unit being considered. Mean fields are related to chemical potentials, and expressions for them include K_ϕ from the entropy of mixing contribution, $w^\circ(p(j))$ from the microscopic thermodynamics characterized by the χ parameters, a contribution Δw associated with the incompressibility constraint, and any additional external fields w_{ext} which may be acting on the

system.[28-30,33,40] For an inhomogeneous system these components are all functions of the position **r**:

$$w(\mathbf{r},j) = w^{\circ}(\mathbf{r},p(j)) - k_B T K_{\phi}(\mathbf{r}) - \Delta w(\mathbf{r}) + w_{ext}(\mathbf{r},p(j)) \quad (41)$$

with

$$\frac{\Delta w(\mathbf{r})}{k_B T} = \zeta\{-\sum_k \phi_k(\mathbf{r}) 1\} \quad (42)$$

Here ζ is inversely proportional to the bulk compressibility of the system. Values of ζ used in the calculations are high enough so that the results obtained are indistinguishable from the incompressible limit corresponding to $\zeta = \infty$. We have also neglected nonlocal terms associated with the long-range nature of the interactions characterized by the χ parameters. These contributions can easily be included, but their contribution is relatively minor and does not affect the results significantly.[41]

The **r** dependencies of the mean fields and volume fractions are expressed in terms of the index i for one-dimensional problems or through i_1 and i_2 for two-dimensional problems. Self-consistent solutions to the set of discretized mean-field equations are obtained numerically by a relaxation method as described previously.[30] Several quantities of interest, including the interfacial tension and the interfacial copolymer excess, are obtained by summing over all lattice sites in the system. Because the lattice represents a specific discretization of a continuum picture, these summations are represented by integrals in the following sections, where specific results from the SCF treatment are presented.

IV. Bulk Micelles

As discussed in section II, bulk micelles appear when the excess free energy associated with their formation vanishes. This excess free energy $\Delta F_{micelle}$ is embodied in the quantity Δw:

$$F_{xs} = \int_{r=0}^{\infty} L(r)\, \Delta w(r) \quad (43)$$

The critical chemical potential for the formation of bulk micelles is the value which gives $\Delta F_{micelle} = 0$ or, alternatively, $\mu_c = F_{micelle}/Q$. In general there will be three solutions to the SCF equations for a given value of μ_c. One is the trivial solution where the composition is completely homogeneous. The remaining two solutions correspond to micelles with two different radii as illustrated in Figure 2a. The solution with the lower radius corresponds to a maximum in $\Delta F_{micelle}$, and the solution with the higher radius corresponds to a minimum in $\Delta F_{micelle}$. The value of μ^b_{cmc} is obtained by iterating μ_c until the high radius solution gives $\Delta F_{micelle} = 0$. This process is simplified by use of a relationship between the size of a micelle and the rate at which $\Delta F_{micelle}$ varies with μ_c. The relationship between these quantities can be derived by defining the quantity V^* as follows:

$$V^* = \int_{r=0}^{\infty} \{\phi_c(r) - \phi_c(\infty)\} L(r) \quad (44)$$

where ϕ_c^{∞} is the copolymer volume fraction in the bulk phase in equilibrium with the micelle. The quantity V^* is the effective volume of a spherical micelle, the effective cross-sectional area for a cylindrical micelle, and the effective thickness of a lamellar micelle. The characteristic size of the micelle is the radius r^* (corresponding to R from the scaling theory), given by

$$r^* = \{V^*/V(1)\}^{1/(3-d)} \quad (45)$$

where d is the dimensionality of the micelle and $V(1)$ is the volume of the first lattice layer. One has $d = 0$ and $V(1) = 4\pi/3$ for spherical micelles, $d = 1$ and $V(1) = 2\pi$ for cylindrical micelles, and $d = 2$ and $V(1) = 2$ for lamellar micelles. We can now write an equation analogous to the Gibbs adsorption equation, where $\Delta F_{micelle}$ is analogous to the interfacial free energy:

$$d(\Delta F_{micelle}) = Q^*\, d\mu_c \quad (46)$$

The copolymer excess Q^* is obtained from V^* by dividing by the volume of a copolymer chain. The quantities $\Delta F_{micelle}$ and Q^* are per spherical micelle, per unit length of a cylindrical micelle, and per unit area of a lamellar micelle. Equation 46 is valid when the bulk copolymer volume fraction ϕ_c^{∞} is very low, so that the homopolymer chemical potential is always close to zero. The value of μ^b_{cmc} is obtained by obtaining values of $\Delta F_{micelle}$ and Q^* from an initial guess for μ^b_c. The quantity Q^* gives the derivative of $\Delta F_{micelle}$ with respect to μ_c according to eq 46. The next guess for μ^b_{cmc} is therefore obtained by adding $\Delta F_{micelle}/Q^*$ to the original guess. This scheme is repeated until subsequent guesses for μ^b_{cmc} differ by less than the desired precision. Three iterations are typically required to obtain a precision of $0.01 k_B T$. The initial estimate of the mean fields must be good enough so that the high radius solution is obtained in each case. The activation free energy for micelle formation is obtained from eq 43, using the low radius solution to the SCF equations with $\mu_c = \mu^b_{cmc}$.

A given copolymer/homopolymer blend system is specified by χN, g, and N_h/N_c. Results obtained from the SCF calculations are independent of the specific values of N_h and N_c used in the calculations, provided that these values are relatively high, that χN, g, and N_h/N_c remain constant, and that all lengths are scaled by R_g.[18,33] All of the calculations presented here were made with values of N_h and N_c which are high enough (>300) so that we are always within this "flexible chain" limit.

Calculated micelle parameters for a series of blend systems are listed in Table I. The equilibrium micellar geometry is the one which gives the lowest value of μ^b_{cmc}. All of the systems listed in Table I have relatively low values of g, and spherical bulk micelles are stable in each case. The systems with $\chi N = 50.5$ and $g = 0.148$ are listed because deuterated polystyrene/poly(2-vinylpyridine) (dPS/PVP) diblock copolymers with these parameters have been extensively studied in polystyrene matrices.[17,26] In these experiments the critical micelle concentration was determined by measuring the depth profile of the diblock copolymers in thin polystyrene matrix films. For $N_h/N_c \gtrsim 1$, bulk micelles form preferentially at the surface of these films. Surface segregation of these micelles is driven by a favorable interaction between the micelle coronas and the free surface of the film. One must be careful to distinguish this situation from the formation of true surface micelles such as those illustrated in Figure 1b, where the

Table I
Micelle Parameters As Calculated by the Self-Consistent-Field Theory

χN	g	N_h/N_c	$\mu^b_{cmc}/k_B T$	ϕ^b_{cmc}	r^*/R_g	geometry
60	0.2	1	5.36	0.0013	2.64	sphere
50.5	0.148	4	5.17	0.055	2.44	sphere
50.5	0.148	2	5.00	0.060	2.39	sphere
50.5	0.148	1	4.67	0.070	2.30	sphere
50.5	0.148	0.5	4.01	0.094	2.10	sphere

surface segregation of copolymer chains is driven by a favorable interaction between the surface and the micelle cores. The favorable corona/surface interactions responsible for the surface segregation of bulk dPS/PVP micelles in a PS matrix can be attributed to the slightly lower surface energy of dPS as opposed to normal PS and to the entropic penalty associated with the distortion of homopolymer matrix chains at the corona/homopolymer interface.[15,17,18] The appearance of a surface copolymer excess of dPS/PVP copolymer chains from a PS matrix phase is therefore an unmistakable signature of micellization from which the critical concentration for the formation of bulk micelles can be determined. As N_h/N_c is increased the micelle parameters reach an asymptotic form for which the results for $N_h/N_c = 4$ are a good approximation. The theoretical value of $5.17k_BT$ for μ^b_{cmc} ($N_h/N_c = 4$) is in excellent agreement with the experimentally determined value of $5.25 \pm 0.5k_BT$ ($N_h/N_c \cong 13$).[17] The magnitude of the trend toward higher values of the critical micelle concentration ϕ^b_{cmc} as N_h/N_c is increased is also in good agreement with experiment.[25] These results suggest that the activation energy for micelle formation ($13k_bT$ for $\mu_c = 5.17k_BT$ as predicted by the SCF theory) could be overcome during the experimental time scale in these experiments. For $N_h/N_c \lesssim 1$, the attractive interactions which give rise to surface segregation of bulk micelles are overwhelmed by repulsive, osmotic interactions arising from the higher entropy of mixing of low molecular weight homopolymer chains.[18] It is therefore not possible to use simple depth profiling techniques to measure the critical micelle concentration for the low values of N_h/N_c, where changes in this ratio are predicted to have a more significant effect on the critical micelle concentration. Other techniques, such as transmission electron microscopy,[42] must be used to determine the critical micelle concentration in this regime.

The SCF theory of micellization can clearly be used to analyze a wide range of transitions in block copolymer/homopolymer blends including, for example, transitions between different micelle geometries with varying N_h/N_c. For very small values of N_h/N_c the treatment reduces to that of copolymer micelles in a small-molecule solvent, a problem which has been treated previously by Yuan et al.[43] The focus of the present paper is on surface phase transitions, however, and for this reason our discussion of micellization is limited primarily to the determination of μ^b_{cmc} as the limiting equilibrium value of the copolymer chemical potential. In order to illustrate some of detailed features of the surface behavior of diblock copolymer/homopolymer blends, we will consider a model blend with $\chi N = 60$, $g = 0.2$, and $N_h/N_c = 1$. The calculated micelle parameters for this system are listed in Table I. Values for μ^b_{cmc} and for the equilibrium micelle size r^{*b}_{cmc} for this system are surprisingly close to the values obtained from the scaling relations for these quantities as given by eqs 10 and 11. The scaling treatment gives $\mu^b_{cmc} = 5.62k_BT$ and $R^b_{cmc} = 2.89R_g$, whereas the detailed SCF treatment gives $\mu^b_{cmc} = 5.36k_BT$ and $r^{*b}_{cmc} = 2.64R_g$. We have compared the SCF results to the scaling predictions for a spherical geometry even though this treatment predicts that cylinders are the preferred geometry for $g > 0.135$. This discrepancy is not surprising, given the approximate nature of the scaling theory and the very small differences between the chemical potentials for spherical and cylindrical micelles as given by eqs 10 and 12.[17] In fact the SCF prediction for μ^b_{cmc} for cylindrical micelles is only slightly higher than the value obtained for spherical micelles: $5.42k_BT$ instead of $5.36k_BT$.

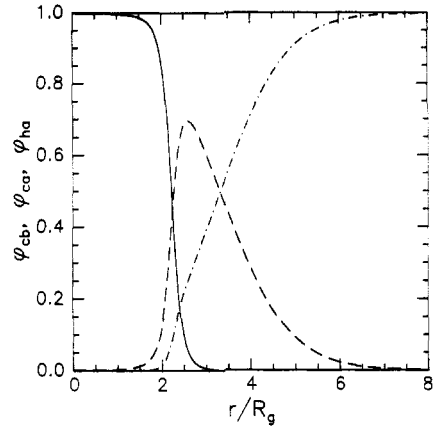

Figure 6. Volume fractions for the core block (—), corona block (– –), and homopolymer (– · –) for a spherical bulk micelle with $g = 0.2$, $\chi N = 60$, and $N_h/N_c = 1.0$.

In addition to being more accurate, the SCF theory gives detailed structural information which is not present in the simple scaling treatment. The volume fractions corresponding to the homopolymer and to the different copolymer blocks for the example system described above are plotted in Figure 6 as a function of the distance from the center of the micelle. The micelle core is very nearly pure copolymer, but there is considerable penetration of the homopolymer chains into the corona. This homopolymer penetration increases substantially as N_h/N_c is decreased to values less than 1 but remains relatively unchanged for higher values of N_h/N_c. This result is consistent with the fact that the structure of a micelle is not strongly dependent on N_h/N_c when this ratio is larger than 1.[18] The results presented here for $N_h/N_c = 1$ are typical of what should be expected for all higher values of this ratio.

V. Surface Micelles

While we expect that the surface phase diagram will have the basic appearance shown in Figure 3, one must use the full SCF treatment in order to predict the location of specific boundaries. In fact there will be a different surface phase diagram for each value of N_h/N_c, with an asymptotic form of the phase diagram being valid for $N_h/N_c \gg 1$. Calculation of the detailed phase diagram from the SCF theory is an enormous task which is beyond the scope of this work. Instead we consider the effects of a surface on our example blend system with $\chi N_c = 60$, $g = 0.2$, and $N_h/N_c = 1$, keeping in mind that micelle formation in the bulk matrix phase limits the copolymer chemical potential to values below $5.36k_BT$. In addition we will consider only values of $\gamma_a - \gamma_b$ which favor the formation of cylindrical surface micelles, allowing us to assume translational invariance in the y direction. One can use the axial symmetry of an isolated spherical micelle to carry out a similar analysis, since this problem is also two-dimensional. The detailed treatment of an array of spherical surface micelles is intrinsically a three-dimensional problem, however, and it is for this reason that we confine our discussion to the treatment of cylindrical surface micelles.

Surface effects are accounted for by introducing an external field $w_{ext}(i_1)$. The effect of a free surface is to introduce a preferential interaction with one of the types of repeat units. For simplicity, we consider the step function potential $w_{ext}(i_1) = w_{ext}(1)\ \delta(i_1 - 1)$ which acts only on repeat units of type B. This simplistic form of the potential acts only in the first layer of width a, where a is the statistical segment length of a repeat unit. Here

$w_{ext}(1)$ is defined as a negative quantity when the B repeat units are attracted to the surface and is analogous to the surface interaction parameter χ_s which has been used in previous treatments.[31,32,44] For a binary blend the quantity $w_{ext}(1)$ represents the free energy decrease associated with the replacement of an A segment in the first lattice layer with a B segment. In accordance with earlier treatments of surface segregation in homopolymer blends[45] and pure diblock copolymer melts,[33,46] we define a bare surface free energy F_s, which is the only component of the surface free energy which is sensitive to the surface composition. The derivative of F_s with respect to ϕ_1, the volume fraction of B repeat units in the first layer, is obtained from $w_{ext}(1)$ by multiplying by the number of segments per unit area which are affected by this external potential:

$$\partial F_s/\partial\phi_1 = a\rho_0 w_{ext}(1) \tag{47}$$

where the width of a single lattice layer is equal to the statistical segment length a of a repeat unit. Note that a and ρ_0 both depend on how a repeat unit is defined. Because this definition is somewhat arbitrary, it is more convenient to work in terms of R_g and v, where v is the volume of a copolymer chain. With $R_g = a(N_c/6)^{1/2}$ and $v = N_c/\rho_0$ we can rewrite eq 47 as follows:

$$\frac{\partial F_s}{\partial\phi_1}\frac{v}{R_g k_B T} = (6N_c)^{1/2} w_{ext}(1) \tag{48}$$

A truly localized surface potential is obtained only in the limit where N_c approaches ∞. We show in the appendix, however, that for homopolymer blends the surface segregation depends only slightly on N_c when N_c is large and the quantity $N_c^{1/2}w_{ext}(1)$ is held constant. Similar universal behavior is observed for systems involving block copolymers.[33] In the discussion which follows we ignore corrections associated with the finite size of a lattice layer and use eq 47 to convert $w_{ext}(1)$ to $\partial F_s/\partial\phi_1$. We ignore the dependence of $\partial F_s/\partial\phi_1$ on ϕ_1 itself, in which case $\partial F_s/\partial\phi_1$ is equivalent to the bare surface free energy difference between A and B homopolymers used in the scaling treatment of section II:

$$-\partial F_s/\partial\phi_1 = \gamma_a - \gamma_b$$

A composition dependence of $\partial F_s/\partial\phi_1$ can easily be included in the calculations, although little is gained for high values of χN_c where a given region on the surface consists of either nearly pure A or nearly pure B.

Because the composition within a cylindrical micelle varies in two dimensions (x and z, where z is the direction normal to the interface), it is impossible to capture the detailed micellar structure in a single plot. The fundamental features of the micelle structure are captured by integrating over the z coordinate to obtain the quantities $z^*_c(x)$ and $z^*_{cb}(x)$:

$$z^*_c(x) = \int_0^\infty (\phi_c(x,z) - \phi_c(x,\infty))\,dz \tag{49}$$

$$z^*_{cb}(x) = \int_0^\infty (\phi_{cb}(x,z) - \phi_{cb}(x,\infty))\,dz \tag{50}$$

The functional forms of $z^*_c(x)$ and $z^*_{cb}(x)$ give an indication of the respective shapes of the overall micelle and of the micelle core. These quantities are functions of only a single spatial coordinate x for the cylindrical micelles considered here. The overall interfacial copolymer excess which would actually be measured in an adsorption experiment is given by the average value of z^*_c. For the cylindrical geometry

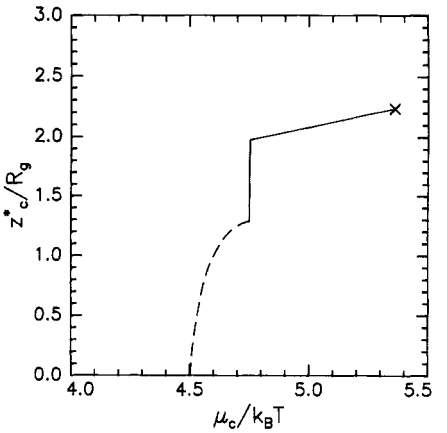

Figure 7. Adsorption isotherm for a copolymer with $g = 0.2$, $\chi N_c = 60$, and $N_h/N_c = 1.0$ at a surface with $-\partial F_s/\partial\phi_1 = 3k_BTR_g/v$.

z^* is given by

$$z^* = \frac{1}{\Lambda}\int_0^\Lambda z^*_c(x)\,dx \tag{51}$$

where Λ is the periodicity of the array of cylindrical micelles. The equilibrium value of Λ for a given value of the copolymer chemical potential is the value which minimizes the excess free energy of the system. This excess free energy is actually the interfacial tension γ which is obtained from Δw. For an array of cylindrical micelles one has

$$\gamma = \frac{\rho_0}{\Lambda}\int_0^\Lambda dx \int_0^\infty \Delta w(x,z)\,dz \tag{52}$$

The equilibrium surface morphology is the one which minimizes γ as given by eq 52.

Results of SCF calculations for our model system with $N_h/N_c = 1$, $g = 0.2$, and $\chi N_c = 60$ are consistent with a phase diagram which has the basic form shown in Figure 3. These calculations indicate that a bare surface free energy difference $\gamma_a - \gamma_b = 3k_BTR_g/v$ places the system in the region denoted CL. As discussed in section II, the appropriate normalization for $\gamma_a - \gamma_b$ is γ_{ab}, the free energy associated with an interface between A-rich and B-rich regions. As an estimate for this quantity we take the interfacial tension between homopolymers of infinite molecular weight as given in eq 6:

$$\gamma_{ab} \approx a\rho_0(\chi/6)^{1/2} = 2(\chi N)^{1/2}R_g k_B T/v \tag{53}$$

One therefore obtains 0.19 as the nominal value of the quantity $(\gamma_a - \gamma_b)/\gamma_{ab}$ for our system with $\chi N_c = 60$ and $\gamma_a - \gamma_b = 3k_BTR_g/v$.

The adsorption isotherm for our model system is shown in Figure 7. The first transition in this adsorption isotherm corresponds to the appearance of cylindrical surface micelles at the critical copolymer chemical potential $\mu^s_{cmc} = 4.5k_BT$ for the formation of these surface micelles. The second transition is from a cylindrical to a lamellar surface morphology at $\mu_c = 4.75k_BT$. Figure 8 shows $z^*_c(x)$ and $z^*_{cb}(x)$ for the cylindrical micelles at the two transition points in the isotherm. The boundary between the A and B regions of the surface of the micelle is quite sharp, so the plot of $z^*_{cb}(x)$ gives what amounts to a cross-sectional view of the micelle core. This cross section is roughly semicircular, as it must be in order for the scaling treatment of section II to remain valid. The SCF treatment captures the detailed shape of this cross section and also gives the equilibrium repeat period Λ of the periodic surface

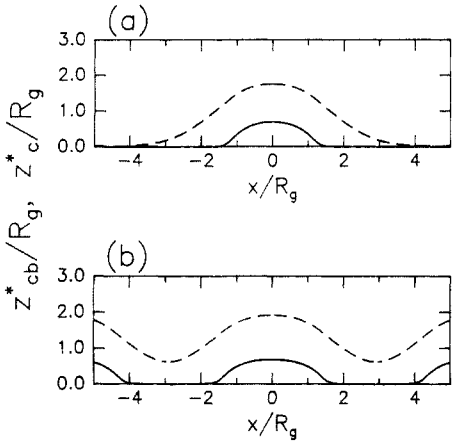

Figure 8. Profiles for the cylindrical surface morphology at the two transition points in the isotherm in Figure 7: (a) μ_c/k_BT = 4.50; (b) μ_c/k_BT = 4.75.

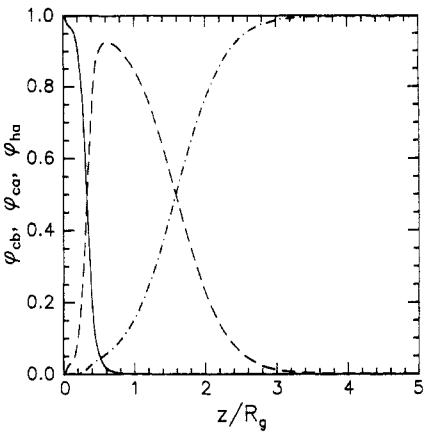

Figure 9. Volume fractions of the adsorbing B block (—), the nonadsorbing A block (– –), and homopolymer (– · –) for the lamellar surface morphology corresponding to the last point on the adsorption isotherm of Figure 7 (μ_c/k_BT = 5.36).

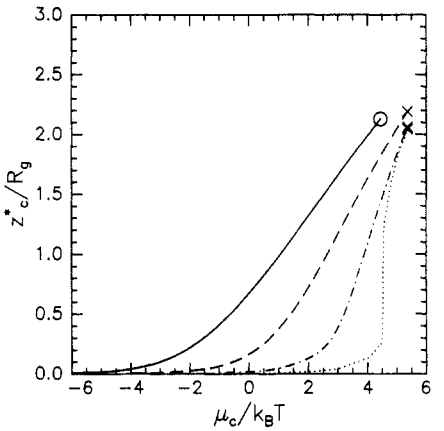

Figure 10. Adsorption isotherms for an A/B diblock copolymer at the interface between A and C homopolymers with g = 0.2, $\chi_{ab}N$ = 60, and $\chi_{ac}N$ = 60. The four curves correspond to $\chi_{bc}N$ = −15 (—), $\chi_{bc}N$ = 0 (– –), $\chi_{bc}N$ = 15 (– · –), and $\chi_{bc}N$ = 30 (· · ·). All three polymers have the same degree of polymerization N.

structure. This repeat period is actually infinite at the surface micelle transition; i.e., the transition is to a collection of isolated cylindrical micelles. When $\mu_c = \mu^s_{cmc}$, the excess free energy associated with the formation of an isolated cylindrical micelle vanishes. Repulsive brush/brush interactions between the coronas of neighboring surface micelles contribute to the free energy, leading to an increase in the free energy of the system with decreasing Λ. Higher values of the copolymer chemical potential favor an increased surface copolymer excess z^*, giving rise to a minimum value of the free energy for a finite value of Λ. The very steep rise in the adsorption isotherm for $\mu_c > \mu^s_{cmc}$ can be attributed to the development of a characteristic intermicellar spacing for copolymer chemical potentials which are only slightly higher than μ^s_{cmc}. Some error exists in the detailed nature of the adsorption isotherm in this regime because of numerical difficulties associated with the determination of the value of Λ which minimizes γ as given by eq 52. This region of the adsorption isotherm is therefore shown as a dashed line in Figure 7. The quantities z^*_{cb} and z^*_c are independent of x for the lamellar surface morphology. Thus, at μ_c = 4.75 the surface morphology undergoes a first-order phase transition from a cylindrical morphology, where $z^*_{cb}(x)$ and $z^*_c(x)$ are periodic, to a lamellar morphology where these quantities are translationally invariant. The z dependences of the volume fractions of the homopolymer and of each copolymer block for the lamellar morphology are plotted in Figure 9.

VI. Copolymers at the Interface between Immiscible Homopolymers

The calculations from the previous section apply to a sharp interface, where the overall polymer density decays from its bulk value to zero over a single lattice layer. These results are representative of what one would obtain at the free surface of a polymer or at a polymer/nonpolymer interface. We turn our attention now to some results for the segregation of an A/B diblock copolymer to an interface between immiscible homopolymers A and C. These results are an extension of an earlier treatment of an A/B diblock copolymer at the interface between A and B homopolymers.[30] Generalization to the case where the blocks do not have the same chemical compositions as the homopolymers has also been considered by Vilgis and Noolandi, although only for situations where a large amount of a nonselective solvent is present.[47] We consider the situation where the block copolymer and each of the homopolymers has the same degree of polymerization N. The respective thermodynamic interactions between A and B repeat units, B and C repeat units, and A and C repeat units are represented by the three interaction parameters χ_{ab}, χ_{bc}, and χ_{ac}. The calculations can of course be carried out in two dimensions to examine the possible formation of laterally heterogeneous surface structures. As discussed briefly at the end of this section, the possible formation of these sorts of structures can often be discounted. Compositional variations in the plane parallel to the homopolymer interface have therefore been ignored in calculations described below.

Adsorption isotherms as calculated by the SCF theory for g = 0.2 and $\chi_{ab}N = \chi_{ac}N$ = 60 are plotted in Figure 10 for $\chi_{bc}N$ = −15, 0, 15, and 30. For values of $\chi_{bc}N$ which are less than some critical value there is a continuous evolution of the copolymer layer with increasing μ_c. These values of $\chi_{bc}N$ correspond to the strong adsorption regime of Figure 3, where no phase transitions are observed in the isotherm. The isotherms have a sigmoidal character, where the central portion of the isotherm gets steeper as $\chi_{bc}N$ is increased. At the critical value of $\chi_{bc}N$ the steepest portion of the isotherm is completely vertical, indicating that two values of z^* are in equilibrium with one another. This critical value of $\chi_{bc}N$ is close to 30 for the parameters corresponding to the isotherms of Figure 10. At higher values of $\chi_{bc}N$ the isotherm consists of a low z^* branch and a high z^* branch. One must compare the free energies of each branch in order to determine the value of μ_c at

which the equilibrium isotherm moves from one branch to the other.

Segregation of block copolymer chains to the interface is driven by the preference for the B copolymer block to exist within or adjacent to the C phase rather than within the A phase. The basic features of this adsorption process for highly asymmetric diblock copolymers and low values of z^* can be understood in the context of polymer brushes. Here the A copolymer block is treated as a brush which is anchored to the interface by the B copolymer block. Following an earlier treatment of block copolymers at homopolymer interfaces,[10] we let $k_BT\chi_e^b$ and $k_BT\chi_e^s$ represent the respective free energies associated with the placement of the B copolymer block in the bulk A phase and at the interface. The overall free energy decrease β (normalized by k_BT) associated with the removal of a B copolymer block from the bulk A phase and its placement at the interface with the C phase is obtained by inclusion of the joint localization term ΔF_{loc}:

$$\beta = \chi_e^b - \chi_e^s - \Delta F_{loc}/k_BT \tag{54}$$

The chemical potential of an adsorbed copolymer chain is given by

$$\mu_c = \Delta F_{loc} + \chi_e^s + \bar{\mu} \tag{55}$$

where $\bar{\mu}$ represents the contribution to the copolymer chemical potential arising from the extension of the A copolymer block into the A homopolymer matrix. The quantity $\bar{\mu}$ depends on z^* and is only weakly dependent on the homopolymer to brush molecular weight ratio when this ratio is larger than 1.[18] The quantity χ_e^b is given by $g\chi_{ab}N$, which is equal to 12 for each of the adsorption isotherms shown in Figure 10. For very low values of z^* the quantity χ_e^s can be approximated as the free energy required to put a B copolymer block in a matrix of C homopolymer:

$$\chi_e^s \approx gN\chi_{bc} \tag{56}$$

Because the quantity μ is a function only of z^* (when the molecular weights remain fixed), the addition of a constant factor C to χ_e^s shifts the adsorption isotherms to lower chemical potentials by an amount equal to k_BTC. This picture is consistent with the behavior of the adsorption isotherms shown in Figure 10, where at very low values of z^* adjacent adsorption isotherms are offset from one another along the abscissa by approximately $3k_BT$. At higher values of z^* eq 56 breaks down, and one can no longer assume that χ_e^s has a simple analytic form. In this regime the adsorption isotherms can be understood by treating χ_e^s as a phenomenological parameter which gives the B block contribution to the overall copolymer chemical potential. As the local concentration of B copolymer segments in the interfacial region increases, χ_e^s approaches zero because the B copolymer segments are being inserted into an environment which consists primarily of identical B polymer segments. In addition there is a positive contribution to χ_e^s associated with entropic stretching of the B copolymer block. Both of these corrections to χ_e^s are minimized for very asymmetric block copolymers[10] but clearly become significant at high values of z^* for $g = 0.2$.

Although it is certainly possible to treat χ_e^s as a phenomenological parameter which varies with z^* as described above, it is perhaps more beneficial to think in terms of the development of separate A/B and B/C interfaces which form when the local volume fraction of the B repeat units becomes quite high. Transitions in the

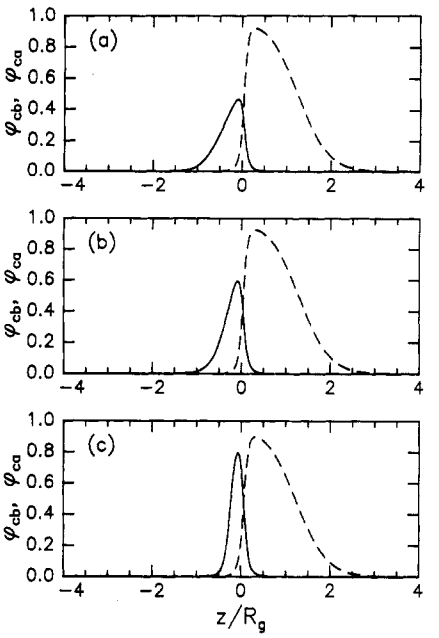

Figure 11. Volume fractions for the A (– –) and B (—) blocks for the end points of three of the adsorption isotherms shown in Figure 10: (a) $\chi_{bc}N = -15$; (b) $\chi_{bc}N = 0$; (c) $\chi_{bc}N = 30$.

adsorption isotherm are possible when the combined free energy of these interfaces exceeds the free energy of the original interface between A and C homopolymers. When these interfaces are fully formed the interfacial excess z^* will depend only on the copolymer chemical potential and not on χ_{bc}. It is essentially for this reason that the values of z^* at the limiting copolymer chemical potential of $5.36k_BT$ (corresponding to the formation of bulk micelles) are nearly identical for all nonnegative values of χ_{bc} shown in Figure 10.

The interfacial tension is obtained from a given calculation by integration of the excess free energy Δw. It can also be obtained from the adsorption isotherms of Figure 10 by making use of the following form of the Gibbs adsorption equation, valid for low copolymer concentrations in the bulk phases:[18]

$$\frac{(\gamma_0 - \gamma(\mu_c))v}{R_g k_B T} = \int_{-\infty}^{\mu_c} \frac{z^*(\mu_c')}{R_g}\, d\mu_c' \tag{57}$$

where $\gamma(\mu_c)$ is the interfacial tension between the A and C homopolymer phases in the presence of block copolymer and γ_0 is the interfacial tension in the absence of block copolymer. The normalized decrease in the interfacial tension is therefore given by the area under the adsorption isotherms shown in Figure 10. Note that for the nonzero values of $g\chi_{ab}N$ the interfacial tension at $\mu_c = 5.36k_BT$ is a strong function of $g\chi_{bc}N$, even though the interfacial structure in each case is similar. The adsorption isotherm for $\chi_{bc}N = -15$ terminates at a copolymer chemical potential of $\mu_c = 4.44k_BT$ because the interfacial tension vanishes at this point; i.e., the decrease in interfacial tension given by eq 57 is equal to γ_0. Addition of copolymer to this system will lead to the formation of an emulsified "droplet phase" consisting of stabilized C homopolymer droplets in an A matrix phase.[9,10,19]

The concentration profiles for A and B copolymer segments for a flat interface for which $\gamma = 0$ are shown in Figure 11a. The profiles for $\chi_{bc}N = 0$ and $\chi_{bc}N = 6$ are shown in parts b and c of this figure, respectively, for $\mu_c = \mu^b{}_{cmc} = 5.36k_BT$. The A block profiles are nearly identical in each case, consistent with the similar z^* values for these three situations. The width of the B block profile is largest

for the negative value of χ_{bc}. This increased width is an example of "enthalpic swelling" of a polymer brush driven by the tendency to maximize the favorable A/B interactions.[48] For positive values of χ_{bc} these interactions are minimized, leading to a compression of the B block profile as shown in Figure 11c.

In concluding this section we briefly consider the possibility of laterally inhomogeneous interface structures for an A/B diblock copolymer at the interface between immiscible homopolymers. These structures can be viewed as the lateral phase separation of a homogeneous layer of the sort depicted in Figure 11. This type of lateral phase separation is of course only possible for $\chi_{bc} > 0$ and is not a factor in the interpretation of previous experimental data where χ_{bc} was zero[17,26] or negative.[10] Laterally heterogeneous interface structures are certainly possible for high values of χ_{bc}. Of course if χ_{bc} exceeds χ_{ac} there will be no interface segregation. In the language of section II we expect these structures to appear when $(\gamma_{ac} - \gamma_{bc})/\gamma_{ab}$ is small and positive. This situation corresponds to the case where χ_{bc} is close to, but not exceeding, χ_{ac}.

Measurement of the interfacial segregation of an A/B diblock copolymer to an interface between A and B homopolymers has been shown to be an effective way of measuring χ_{ab}.[17,26] Measurements of A/B diblock copolymer segregation to an interface between A and C or B and C homopolymers may provide a means by which χ_{ac} and χ_{bc} can be obtained. The technique is particularly powerful because A/C and B/C diblock copolymers are not required for the experiment. The technique is straightforward when large negative values of χ_{bc} are involved, since very asymmetric block copolymers can be used and the interface segregation can be interpreted in terms of χ_e^s as given by eq 54.[10] The situation is complicated when all of the χ parameters are positive, as is generally the case. In these situations comparison should be made to the detailed adsorption isotherms as predicted by the SCF theory while taking into account the possibility of laterally heterogeneous interface structures.

VII. Summary

We have shown that laterally heterogeneous surface structures can be formed when an A/B diblock copolymer adsorbs to a surface from an A homopolymer melt. The fundamental physics which lead to the appearance of these structures are described by a scaling theory of micellization. The presence of a surface which has a preferential interaction with the B polymer segments leads to the formation of an adsorbed copolymer layer at values of the copolymer chemical potential which are lower than the value corresponding to the formations of bulk micelles within the homopolymer matrix phase. Strong surface attractions favor the formation of a laterally homogeneous lamellar copolymer layer of the sort which is typically assumed. Cylindrical or spherical surface micelles are predicted to appear however, for asymmetric block copolymers where the B block is only weakly adsorbing. Higher copolymer chemical potentials favor the formation of more homogeneous surface structures, and certain regimes are predicted where transitions between spherical and cylindrical or between cylindrical and lamellar surface morphologies will occur as the block copolymer chemical potential is increased.

Quantitative features of these heterogeneous surface morphologies and the transitions between them are obtained from a two-dimensional self-consistent-field theory, where composition variations perpendicular to the interface and within the plane of the interface are allowed. Model calculations indicate that the fundamental features of the scaling model are indeed correct. In particular, it appears that it is valid to think in terms of surface micelles which are roughly spherical, cylindrical, or lamellar. Morphologies which are intermediate between these cases, i.e., spheres or cylinders which are significantly "flattened", appear to have a higher free energy and are not thermodynamically stable. As a result the first-order character of the transitions between the various surface morphologies is retained. This result was illustrated for a system which showed a transition to a cylindrical morphology at the critical copolymer chemical potential for the formation of surface micelles, followed by a first-order transition to a laterally homogeneous lamellar surface morphology. Comparisons to experimental results, where the equilibrium copolymer concentration in the bulk phase is a measure of the copolymer chemical potential, should allow weak surface interactions to be measured.

A very important aspect of this work concerns the extension of the self-consistent-field theory to the consideration of block copolymer micelles which form in the bulk homopolymer matrix phase. The theory gives values for the equilibrium copolymer chemical potential corresponding to the formation of these bulk micelles which are in quantitative agreement with recent experimental measurements. This limiting copolymer chemical potential μ^b_{cmc} is a very important number, since in many cases the copolymer concentration corresponding to μ^b_{cmc}, i.e., the critical micelle concentration, is very low. In real situations it can often be assumed that the copolymer concentration is larger than the critical micelle concentration, in which case the equilibrium copolymer chemical potential will be closely approximated by μ^b_{cmc}. One can then use this value of the copolymer chemical potential to determine which surface morphology will be present (at equilibrium) for a given surface interaction. The activation free energy for the formation of a bulk micelle can be obtained from the SCF theory as well. This quantity is expected to play an important role in that it can lead to effective copolymer chemical potentials which are higher than the equilibrium value. In addition to providing useful information with regard to the nature of polymer/surface interactions, it is expected, therefore, that studies of the various surface morphologies and the transitions between them will yield useful insights into the kinetics of copolymer aggregation.

Appendix: Properties of Homopolymer Blends

Here we briefly consider some of the properties of symmetric homopolymer blends ($N_a = N_b = N$) as the limiting case where the copolymer symmetry parameter g is equal to 1. Results are compared to predictions from square gradient, or Cahn–Hilliard theory, where the free energy density of an inhomogeneous blend system is approximated as follows:[49]

$$f \cong \int_{-\infty}^{\infty} \{f_0(\phi) + \kappa(\phi)(\partial\phi/\partial x)^2\}\, dz \qquad \text{(A1)}$$

where $\phi \equiv \phi_b(z)$ and $f_0(\phi)$ is given by the Flory–Huggins form of the free energy density of a homogeneous system as given by eq 23. The right-hand side of eq A1 includes only the leading terms in what is actually an expansion of the free energy density in terms of derivatives of ϕ. For infinite molecular weight polymers the coefficients of the higher order derivative terms vanish and eq A1 becomes

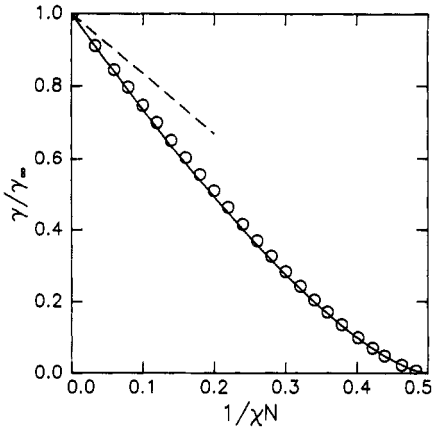

Figure 12. Molecular weight dependence of the interfacial tension between immiscible homopolymers of equivalent molecular weight, as determined by the self-consistent-field theory (symbols). The solid and dashed lines correspond to eqs A3 and A4, respectively.

an equality, with the coefficient of the square gradient term given by κ_∞:[50,51]

$$\kappa_\infty(\phi) = \frac{k_B T \rho_0 a^2}{k\phi(1-\phi)} \tag{A2}$$

with $k = 24$. A similar form for κ is obtained for very broad interfaces which have $d\phi/dz \ll R_g^{-1}$. In this regime the higher order terms can be neglected because the higher order derivatives are themselves negligible. Equation A1 can again be treated as an equality, with κ having the same form as is shown in eq A2, but with $k = 36$.[52]

Interfacial Tension of a Symmetric Immiscible Blend System. For a symmetric system the free energy of mixing expression (eq 23) dictates that there will be a critical point at $\phi = 0.5$ and $\chi N = 2$. The interfacial tension γ between A and B homopolymers of equivalent molecular weight vanishes, therefore, at $\chi N = 2$. For $\chi N = \infty$ an analytic solution can be obtained from the SCF equations of section III or from minimization of the free energy functional given by eqs A1 and A2, with $k = 12$. Both treatments give $\gamma_\infty = a\rho_0 k_B T(\chi/6)^{1/2}$ as given in eq 6.[24,50]

The manner in which γ varies between 0 and γ_∞ for values of χN between 2 and ∞ is shown in Figure 12. The symbols represent the numerical solution of the SCF equations of section III, and the solid line is the following approximate form suggested by Tang and Freed:[51]

$$\gamma/\gamma_\infty = \left\{1 - \frac{1.8}{\chi N} - \frac{0.4}{(\chi N)^2}\right\}^{3/2} \tag{A3}$$

The dashed line is the following result (valid for high values of χN) obtained by Broseta et al.[50] from the minimization of the free energy functional given by eqs A1 and A2 with $k = 24$:

$$\gamma/\gamma_\infty = 1 - \pi^2/6\chi N \tag{A4}$$

The discrepancy between this prediction and the numerical solution of the SCF equations can be attributed to the failure of the simple form of the free energy functional when $d\phi/dz$ becomes comparable to R_g^{-1}. Tang and Freed have pointed out that there is no simple free energy functional in this regime.[51] Their estimate of the interfacial tension as given by eq A3 is merely the simplest form which is consistent with the requirements that $\gamma/\gamma_\infty = 1$ at $\chi N = \infty$ and that the correct weak segregation results[53] be obtained for $\chi N \approx 2$.

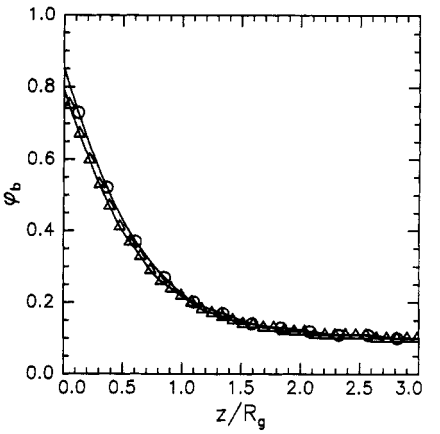

Figure 13. Volume fraction of homopolymer B near the surface of a symmetric homopolymer blend with $\chi = 0$, as determined by the self-consistent-field theory for $\phi_\infty = 0.1$ and $-\partial F_s/\partial\phi_1 = 3k_B T R_g/v$. Data for $N = 100$ (○) and $N = 800$ (△) are included.

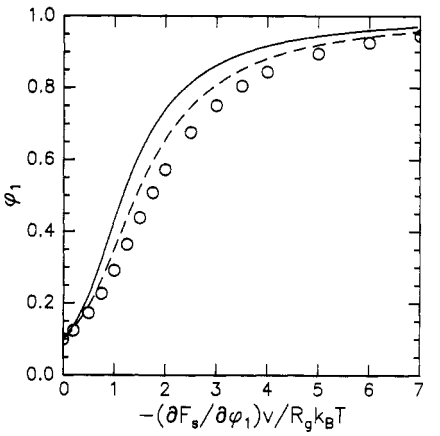

Figure 14. Surface volume fraction ϕ_1 as a function of $-\partial F_s/\partial\phi_1$ for a symmetric polymer blend with $\chi = 0$ and $\phi_\infty = 0.1$. Symbols represent the self-consistent-field results for $N = 800$. The dashed line represents the solution obtained from square gradient theory with $k = 36$, obtained by the procedure outlined by Schmidt and Binder.[45]

Surface Segregation in a Miscible Homopolymer Blend. Figure 13 shows the calculated concentration profiles for a symmetric blend system with $\chi = 0$ in the vicinity of a surface which has a preferential interaction with the B repeat units. The chemical potentials of the homopolymers were fixed by specifying that the equilibrium volume fraction ϕ_∞ of homopolymer B in the bulk be equal to 0.1. The surface interaction $-\partial F_s/\partial\phi_1$ is equal to $3k_B T R_g/v$ for each of the profiles shown in Figure 13, but one curve has $N = 100$ and the other curve has $N = 800$. The largest value which can realistically be chosen for N is the value which gives a statistical segment length a approximately equal to the persistence length of the polymer. The difference between the two curves in Figure 13 is small, indicating that lattice artifacts do not significantly affect the results of the self-consistent-field calculation for highly flexible chains for which values of $N > 100$ can be chosen.

A bare surface free energy can be added to the free energy expression given by eq A1 to calculate the relationship between ϕ_1 and $\partial F_s/\partial\phi_1$. The results of this calculation as described by Schmidt and Binder[45] are represented by the solid and dashed lines in Figure 14, for a symmetric homopolymer blend with $\phi_\infty = 0.1$. The two lines are obtained from the two asymptotic forms of the square gradient term with $k = 36$ for the solid line and $k = 24$ for the dashed line. The symbols represent ϕ_1 as determined

from the SCF theory, where we have taken ϕ_1 as the B volume fraction in the first layer of a system with $N = 800$. Square gradient theory overestimates the surface volume fraction, regardless of which value of k is used. The smaller value of k comes closer to representing the relationship between ϕ_1 and $\partial F_s/\partial\phi_1$, but this value fails to capture the behavior of the tail of the concentration profile, where ϕ decays slowly and we must use $k = 36$. As with the homopolymer interfacial tension, the differences between the square gradient and self-consistent-field predictions can be attributed to the approximate nature of eqs A1 and A2 in the regime where the magnitude of the slope of the concentration profile is comparable to R_g^{-1}.

References and Notes

(1) Tassin, J. F.; Siemens, R. L.; Tang, W. T.; Hadziioannou, G.; Swalen, J. D.; Smith, B. A. *J. Phys. Chem.* **1989**, *93*, 2106.
(2) Munch, M. R.; Gast, A. P. *J. Chem. Soc., Faraday Trans.* **1990**, *86*, 1341.
(3) Munch, M. R.; Gast, A. P. *Macromolecules* **1990**, *23*, 2313.
(4) Hadziioannou, G.; Patel, S.; Granick, S.; Tirrell, M. *J. Am. Chem. Soc.* **1986**, *108*, 2869.
(5) Russel, W. B.; Saville, D. A.; Schowalter, W. R. *Colloidal Dispersions*; Cambridge University Press: Cambridge, U.K., 1989.
(6) Fayt, R.; Jerome, R.; Teyssie, P. *J. Polym. Sci., Polym. Phys. Ed.* **1982**, *20*, 2209.
(7) Brown, H. R. *Macromolecules* **1989**, *22*, 2859.
(8) Creton, C.; Kramer, E. J.; Hui, C.-H.; Brown, H. R. *Macromolecules* **1992**, *25*, 3075.
(9) Wang, Z.-G.; Safran, S. A. *J. Phys. (Fr.)* **1990**, *51*, 185.
(10) Shull, K. R.; Kellock, A. J.; Deline, V. R.; MacDonald, S. A. *J. Chem. Phys.* **1992**, *97*, 2095.
(11) Ligoure, C. *Macromolecules* **1991**, *24*, 2968.
(12) Hasegawa, H.; Hashimoto, T. *Polymer* **1992**, *33*, 475.
(13) Calistri-Yeh, M.; Kramer, E. J.; Sharma, R. *Bull. Am. Phys. Soc.* **1992**, *37*, 517.
(14) Mayes, A. M.; Olvera de la Cruz, M. *Macromolecules* **1988**, *21*, 2543.
(15) Shull, K. R.; Winey, K. I.; Thomas, E. L.; Kramer, E. J. *Macromolecules* **1991**, *24*, 2748.
(16) Winey, K. I.; Fetters, L. J.; Thomas, E. L. *Macromolecules* **1992**, *25*, 2645.
(17) Shull, K. R.; Kramer, E. J.; Hadziioannou, G.; Tang, W. *Macromolecules* **1990**, *23*, 4780.
(18) Shull, K. R. *J. Chem. Phys.* **1991**, *94*, 5723.
(19) Leibler, L. *Makromol. Chem., Macromol. Symp.* **1988**, *16*, 1.
(20) Marques, C. M.; Joanny, J. F.; Leibler, L. *Macromolecules* **1988**, *21*, 1051.
(21) Marques, C. M.; Joanny, J. F. *Macromolecules* **1989**, *22*, 1454.
(22) Semenov, A. N. *Sov. Phys. JETP* **1985**, *61*, 733.
(23) Leibler, L.; Orland, H.; Wheeler, J. C. *J. Chem. Phys.* **1983**, *79*, 3550.
(24) Helfand, E.; Tagami, Y. *Polym. Lett.* **1971**, *9*, 741.
(25) Semenov, A. N. *Macromolecules* **1992**, *25*, 4967.
(26) Dai, K. H.; Kramer, E. J.; Shull, K. R. *Macromolecules* **1992**, *25*, 220.
(27) *Polymer Phase Separation*; Sanchez, I. C., Ed.; Academic Press: Orlando, FL, 1987.
(28) Evers, O. A.; Scheutjens, J. M. H. M.; Fleer, G. J. *Macromolecules* **1990**, *23*, 5221.
(29) Hong, K. M.; Noolandi, J. *Macromolecules* **1981**, *14*, 727.
(30) Shull, K. R.; Kramer, E. J. *Macromolecules* **1990**, *23*, 4769.
(31) Scheutjens, J. M. H. M.; Fleer, G. J. *J. Phys. Chem.* **1979**, *83*, 1619.
(32) Scheutjens, J. M. H. M.; Fleer, G. J. *J. Phys. Chem.* **1980**, *84*, 178.
(33) Shull, K. R. *Macromolecules* **1992**, *25*, 2122.
(34) Leermakers, F. A. M.; Scheutjens, J. M. H. M. *J. Phys. Chem.* **1989**, *93*, 7417.
(35) Edwards, S. F. *Proc. Phys. Soc. London* **1965**, *85*, 613.
(36) Helfand, E.; Tagami, Y. *J. Chem. Phys.* **1972**, *56*, 3592.
(37) Helfand, E. *Macromolecules* **1975**, *8*, 552.
(38) Helfand, E. *J. Chem. Phys.* **1975**, *62*, 999.
(39) Helfand, E.; Wasserman, Z. R. *Macromolecules* **1976**, *9*, 879.
(40) Helfand, E.; Tagami, Y. *J. Chem. Phys.* **1972**, *57*, 1812.
(41) Helfand, E.; Sapse, A. M. *J. Chem. Phys.* **1975**, *62*, 1327.
(42) Kinning, D. J.; Thomas, E. L.; Fetters, L. J. *J. Chem. Phys.* **1989**, *90*, 5806.
(43) Yuan, X.-F.; Masters, A. J.; Price, C. *Macromolecules* **1992**, *25*, 6876.
(44) Hariharan, A.; Kumar, S. K. *Macromolecules* **1991**, *24*, 4909.
(45) Schmidt, I.; Binder, K. *J. Phys. (Fr.)* **1985**, *46*, 1631.
(46) Fredrickson, G. H. *Macromolecules* **1987**, *20*, 2535.
(47) Vilgis, T. A.; Noolandi, J. *Makromol. Chem., Macromol. Symp.* **1988**, *16*, 225.
(48) Brown, H. R.; Char, K.; Deline, V. R. *Macromolecules* **1990**, *23*, 3383.
(49) Cahn, J. W.; Hilliard, J. E. *J. Chem. Phys.* **1958**, *28*, 258.
(50) Broseta, D.; Fredrickson, G. H.; Helfand, E.; Leibler, L. *Macromolecules* **1990**, *23*, 132.
(51) Tang, H.; Freed, K. F. *J. Chem. Phys.* **1991**, *94*, 6307.
(52) Tang, H.; Freed, K. F. *J. Chem. Phys.* **1991**, *94*, 1572.
(53) Joanny, J. F.; Leibler, L. *J. Phys. (Fr.)* **1978**, *39*, 951.